Impact of silica nanoparticle surface chemistry on protein corona formation and consequential interactions with biological cells

Andréa Kurtz-Chalot, Christian L. Villiers, Jérémie Pourchez, Delphine Boudard, Matteo Martini, Patrice Marche, Michèle Cottier, Valérie Forest

Impact of silica nanoparticle surface chemistry on protein corona formation and consequential interactions with biological cells

Andréa Kurtz-Chalot[a,b,c], Christian Villiers[d,e], Jérémie Pourchez[a,b,c], Delphine Boudard[b,c,f,g], Matteo Martini[h], Patrice N. Marche[d,e], Michèle Cottier[b,c,f,g] and Valérie Forest[a,b,c*].

[a] Ecole Nationale Supérieure des Mines de Saint-Etienne, CIS-EMSE, SAINBIOSE, F-42023 Saint Etienne, France.

[b] INSERM, U1059, F-42023 Saint Etienne, France.

[c] Université de Lyon, F-69000 Lyon, France.

[d] Centre de Recherche INSERM U1209, F-38700 La Tronche, France

[e] Université Grenoble-Alpes, Institut Albert Bonniot, F-38700 La Tronche, France.

[f] Université Jean Monnet, F-42023 Saint-Etienne, France.

[g] CHU de Saint-Etienne, F-42055 Saint-Etienne, France.

[h] Institut Lumière Matière, UMR5603 CNRS, Université Claude Bernard Lyon 1, F-69622 Villeurbanne, France.

* Corresponding author: Valérie Forest:

Ecole Nationale Supérieure des Mines de Saint-Etienne

Center for biomedical and healthcare engineering

158 cours Fauriel – CS 62362, 42023 Saint-Etienne Cedex 2, France.

Email address: vforest@emse.fr - Telephone number: +33477499776

Graphical abstract

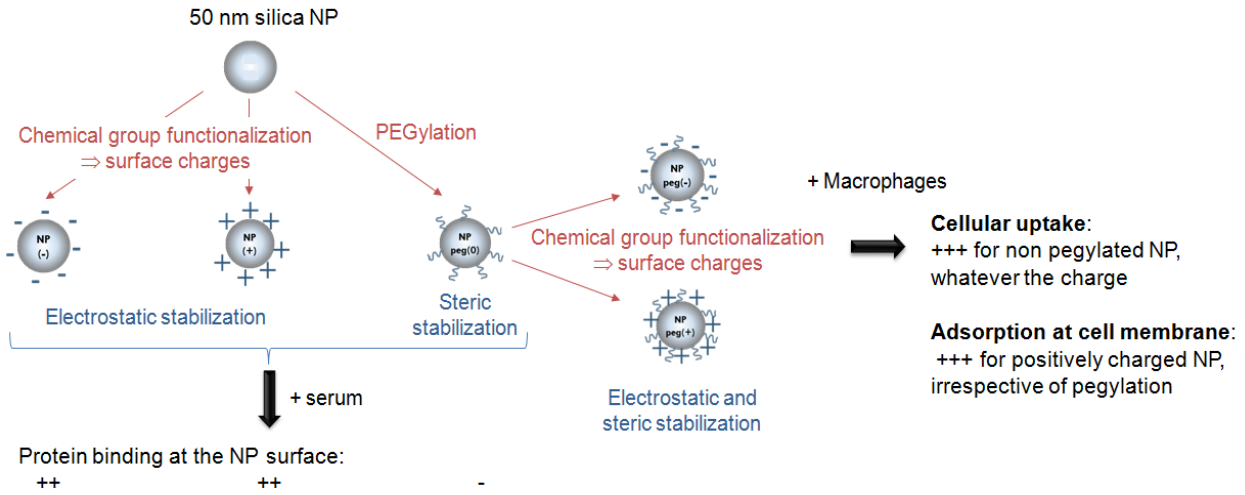

⇒ **Key role of surface chemical functionalization in NP/cells interactions and in the formation of the protein corona.**

ABSTRACT

Nanoparticles (NP) physico-chemical features greatly influence NP/cell interactions. NP surface functionalization is often used to improve NP biocompatibility or to enhance cellular uptake. But in biological media, the formation of a protein corona adds a level of complexity. The aim of this study was to investigate *in vitro* the influence of NP surface functionalization on their cellular uptake and the biological response induced. 50nm fluorescent silica NP were functionalized either with amine or carboxylic groups, in presence or in absence of polyethylene glycol (PEG). NP were incubated with macrophages, cellular uptake and cellular response were assessed in terms of cytotoxicity, pro-inflammatory response and oxidative stress. The NP protein corona was also characterized by protein mass spectroscopy. Results showed that NP uptake was enhanced in absence of PEG, while NP adsorption at the cell membrane was fostered by an initial positively charged NP surface. NP toxicity was not correlated with NP uptake. NP surface functionalization also influenced the formation of the protein corona as the profile of protein binding differed among the NP types.

KEYWORDS

Silica nanoparticles; surface functionalization; cellular uptake; phagocytic cells; protein corona; cytotoxicity.

1. INTRODUCTION

Nanoparticles (NP) represent promising tools for biomedical applications as they can be used as therapeutic and/or diagnostic agents. Their surface can be modified to foster NP/cell interactions and thus enhance their subsequent cellular uptake to reach their intracellular targets [1]. Indeed, NP/cell interactions strongly depend on the NP physico-chemical features and 8 parameters seem to have a crucial importance as defined by ISO/TS 80004-2:2015: agglomeration/aggregation state, composition, size, shape, solubility/dispersibility, specific surface area, density of surface groups and surface chemistry [2,3]. In particular surface charge is recognized to play a major role and it is commonly acknowledged that positively charged NP are more internalized by cells than neutral or negatively charged NP [1,4–10]. A correlation between the amount of positive charges and cellular uptake has even been observed [8]. Consequently, NP surface functionalization by modifying surface charge is an efficient and easy way to drive cellular uptake [5–7,11]. The modulation of the NP physico-chemical features is important not only for the enhancement of cellular uptake but also for the induced biological response (and the potential cytotoxicity) [3,8,12,13]. It is thus crucial to define accurate physico-chemical parameters to take into consideration to manufacture NP with a "safer by design" approach [14]. For example, Nabeshi *et al.*, reported that the reduction of cell proliferation of macrophages was more important when cells were incubated with unmodified silica NP than with the same NP functionalized with amine or hydroxyl groups [15]. Therefore, one easy way to increase NP biocompatibility and enhance their cellular uptake is through surface functionalization. In this context, amorphous silica is a particularly interesting material because the chemistry of the silanes allows surface modification of silica NP with chemical functional groups like specific antibodies (targeting to cancer cells and drug delivery) or fluorescent labels (tumor labeling) [16,17].

But an additional level of complexity should be considered when NP are in contact with biological fluids. Indeed, in these conditions NP are surrounded by a wide variety of biomolecules, especially proteins, which rapidly adsorb at their surface and entirely cover it. This so-called protein corona modifies the original NP physico-chemical features and constitutes the first contact of the nanomaterial with the cells and may influence the biological responses [18–26]. Various strategies may be used to decrease protein adsorption at the NP surface, one consists of the grafting of linear chains of hydrophilic polymers, such as polyethylene glycol (PEG) at NP surface. This process allows reducing protein adsorption by blocking protein-binding sites and creating a steric hindrance [27]. Moreover, the relative density of each type of adsorbed proteins is known to depend on PEG grafting density [28]. The formation of the protein corona is a dynamic process that depends, among others, on nature of the environment and on the NP physico-chemical properties and especially surface charge [18,20,23,29]. It has been shown that increasing the surface charge of NP resulted in a protein adsorption increase in general and of negatively charged serum proteins in particular [4,18,30]. Due to the discrepancy in the published results, the relationship between protein adsorption on NP and the decrease of the cellular internalization of NP remains to be established. Indeed, some studies show that protein adsorption on NP decreases their cellular uptake while other tend to demonstrate the opposite [18,19,25,29–32]. Furthermore, it is difficult to draw firm conclusions from results dealing with different NP types, different functionalization groups, different cellular models, different biological assays, etc. To bring new insights to this issue we propose the present study which aim was to investigate *in vitro* the influence of the functionalization of NP on their cellular uptake and the subsequent biological response. For that purpose, fluorescent silica-based NP were functionalized with chemical groups of different charges in presence or not of a steric hindrance generated by PEG chains. These NP were incubated with macrophages and the cellular uptake was assessed

by fluorimetry. Cellular cytotoxicity, secretion of inflammatory factors and oxidative stress were also evaluated. A major asset of this work is that NP were synthesized in similar conditions and the biological activity was also assessed in the same experimental conditions, limiting variability and allowing reproducible and trustable results. In addition, a study on the influence of the NP surface functionalization on the formation of the protein corona was carried out.

2. EXPERIMENTAL

2.1. Nanoparticle synthesis

Silica-based NP were prepared according to a method developed by Martini *et al.* [33]. The water/oil (W/O) microemulsion procedure was used to produce homogeneous and reproducible core-shell samples. Indeed, reverse micelle (aqueous droplets sized ~10 nm) acts as template for the controlled-growth of core-shell structures. Quaternary W/O microemulsions were prepared by mixing Triton X-100 (surfactant), n-hexanol (co-surfactant) and cyclohexane (oil), followed by sequential additions of specific polar-like precursors. An inclusion of gold clusters at the center of each particle was obtained by the reduction of gold salt in presence of ligands and NaBH4. Please note that although NP contained a gold core, we mainly considered them as made of silica as gold is tightly enclosed in the silica shell. Moreover, assays of stability allowed concluding to the stability of the NP as no dissolution of the silica shell was observed over time. The formation of polysiloxane matrix arose from the base-catalyzed hydrolysis and condensation of two silica precursors: 92 %w TEOS (tetraethoxysilane) and 8%w dye conjugated-APTES ((3-aminopropyl)triethoxysilane). APTES conjugates ensured a covalent bonding of dyes (FITC) and their random distribution within NP. The colloidal stabilization was then achieved by addition of silane precursors with amine or carboxylic acid groups grafted determining the surface charge (Table 1). Thereafter,

all solvents were eliminated by the addition of acetone followed by several cycles of vortexing and centrifuging. Unreacted dyes and precursors were removed by ultrafiltration using 300 kDa PES membranes. Particles were dispersed in aqueous solution (2g/L) and stored at 4˚C.

2.2. Nanoparticle physico-chemical characterization

Scanning electron microscopy (SEM) images of NP were performed using an ESEM XL30-FEI microscope equipped with a thermal field emission gun (FEG). NP samples were prepared by depositing a drop of diluted colloidal solution onto a carbon grid (200 meshes), the solvent was allowed to evaporate at room temperature. Samples were observed under vacuum. Transmission electron microscopy (TEM) images were obtained using a Philips CM200 microscope at a 200 kV accelerating voltage. The size distribution of NP and their zeta potential (ζ) were determined using the nano Zetasizer apparatus (Malvern) based on dynamic light scattering measurement. Measures were performed both in distilled water and in cell culture medium DMEMc (Dulbecco's Modified Eagle's Medium, Invitrogen, Cergy Pontoise, France) supplemented with 10% of fetal calf serum (Invitrogen), 1% penicillin–streptomycin (penicillin 10,000 units/mL, streptomycin 10 mg/mL; Sigma-Aldrich, Saint-Quentin Fallavier, France).

2.3. Cell culture

RAW 264.7 cell line derived from mice peritoneal macrophages transformed by the Abelson murine leukemia virus and was provided by ATCC Cell Biology Collection (Promochem, LGC, Molsheim, France). Cells were cultured in DMEMc at 37°C under a 5% carbon dioxide humidified atmosphere.

2.4. Nanoparticle/cell contacts

For cellular uptake and cytotoxicity assays, cells were seeded in 96-well-plates (100 000 cells in 200µL of medium per well) and were allowed to adhere for 4 h. NP were diluted in cell culture medium to reach the following final concentrations: 75, 750, 4500 and 9000 NP/cell (corresponding to 5, 50, 300 and 600 µg NP/mL respectively). NP were added to cells and further incubated for 20h. Note that for the study of the NP distribution, it seems more relevant to express the NP dose as a number per cell, it seems more explicit, whereas for the cytotoxicity assessments the more relevant unit was µg/mL to ease comparison with literature studies.

2.5. Cellular uptake assessment

Uptake of FITC-labeled NP was quantified using a fluorometer (Ex: 485 nm, Em: 538 nm, Fluoroskan Ascent, Thermolabsystems, France). The total fluorescence of NP was first measured in each well, then the fluorescence of NP in supernatant (1), adsorbed to cell membrane (2) and internalized by cells (3) were discriminated by a "trypan blue (TB) quenching" as previously described [34–38]. TB is known for its ability to "turn off" the green fluorescence emitted by FITC allowing the discrimination of internalized NP from those adhering to plasma membrane [39]. Control wells without NP were used to assess the autofluorescence of cells in culture medium.

2.6. Cytotoxicity assays

Cell membrane integrity – The cellular release in the supernatant of cytoplasmic lactate dehydrogenase (LDH) was assessed using the CytoTox-96™ Homogeneous Membrane Integrity Assay (Promega, Charbonnières-les-Bains, France) according to the manufacturer's instructions. The optical density of the samples was determined using a microplate reader

(Multiskan RC; Thermolabsystems, Helsinki, Finland) set to 450 nm. The activity of the released LDH was reported to that of control cells (incubated without NP). A positive control consisted of the cellular LDH released after cells lysis.

Pro-inflammatory effect – After incubation with NP, the production of Tumor Necrosis Factor α (TNFα) was assessed in the supernatant using a commercial ELISA Kit (Quantikine® Mouse TNFα Immunoassay; R&D Systems, Lille, France) according to the manufacturer's instructions. The optical density of each sample was determined using a microplate reader (Multiskan RC; Thermolabsystems, Helsinki, Finland) set to 450 nm. A standard curve was established, and results were expressed in picograms per milliliter of TNFα. Each experiment included controls: cells incubated alone (negative control) and in presence of DQ12 quartz (positive control) [40,41].

Oxidative stress – A large array of reactive oxygen species (ROS) activity can be assessed with the OxiSelect™ ROS Assay Kit (Euromedex, Mundolsheim, France). The assay uses the conversion of a non-fluorescent substrate, 2.7′-dichlorodihydrofluorescein diacetate that can easily diffuse through cell membranes and be converted into a fluorogenic molecule 2′.7′-dichlorodihydrofluorescein (DCF) in presence of ROS: fluorescence amount is directly related to ROS level. Fluorescence was detected using a Fluoroskan Ascent fluorometer (Ex: 480 nm, Em: 530 nm, Thermolabsystems), and the generation of ROS was expressed as nanomolar using a standard curve previously established.

Statistical analysis – Analysis and graphics were performed on Prism 5.0 software (GraphPad, San Diego, CA). Significance was established with Bonferroni's Multiple Comparison Test. A two-way-ANOVA test was used to compare experimental groups to the negative control (cells incubated without NP). A one-way-ANOVA test was used to compare experimental groups to each other. Data were considered significant when $p<0.05$. Each data

point represents the mean of at least three independent experiments, each carried out in triplicate, and is presented with the arithmetic standard error of the means (± s.e.m).

2.7. Characterization of the protein corona

To determine the influence of the NP surface functionalization on the corona, NP were incubated for 90 minutes with human serum (2.3g/1.3 mL, EFS, Grenoble) to mimic a physiological contact with biological fluids. After 3 washings (1 mL) in PBS à 4°C, 2 in water and 3 in PBS, proteins were desorbed from the NP surface in reductive conditions (dithiothreitol) in presence of a detergent (100µL in Laemmli medium containing SDS). Proteins were sorted depending on their molecular weight by electrophoresis (10% polyacrylamide). After Coomassie Blue staining, all the gel was cut into 25 successive bands that were digested by trypsin. Peptides were extracted using formic acid (1%, v/v) and analyzed by nanoLC-MS/MS (nano-HPLC reverse phase: U3000, Dionex and a 4000 QTRAP: ABSciex). Proteins identification was realized using ProteinPilot (v4.0.8085) with Paragon algorithm and uniprot database.

3. RESULTS

3.1. Nanoparticle characterization

As illustrated in Figure 1A, the NP were spherical and had all the same size (50-55 nm) except NP(+) which were slightly larger (68 nm). The spherical shape could also be clearly observed by TEM as shown in Figure 1B where the dark gold core and the gray silica shell could easily be distinguished.

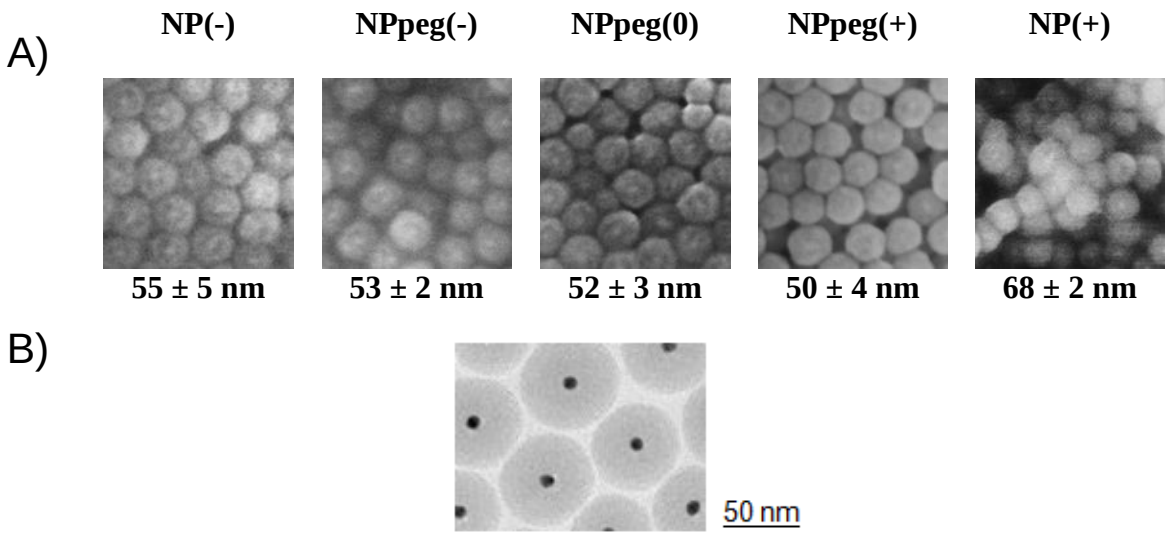

Figure 1 – A) Nanoparticle geometric diameter measured using scanning electron microscopy. Results are means of 30 measures, the standard error is also indicated. B) TEM image of the nanoparticles.

Hydrodynamic diameters and zeta potentials were measured using dynamic light scattering (DLS) both in water and in DMEMc. Data are reported in Table 1. In water and for each type of NP, the hydrodynamic diameter was correlated with the geometric diameter, whereas in culture medium it was significantly increased. Similarly, zeta potentials of the five kinds of NP were distinct in water and coherent with expected values depending on the surface functionalization, whereas in culture medium all zeta potentials were negative. The largest surface charges decrease was observed for the NP without PEG: NP(-) and NP(+).

Table 1 - Nanoparticle physico-chemical characteristics. PDI= polydispersity index, SD= standard deviation.

	Schematic representation	Functionalization	Zeta potential in water (pH7-8)	Zeta potential in DMEMc (pH7-8)	Hydrodynamic diameter (DLS) in water [PDI±SD]	Hydrodynamic diameter (DLS) in DMEMc [PDI±SD]
NP(-)	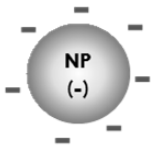	COOH	-42 mV	-135 mV	87±3 nm [0.5±0.005]	110±0 nm [0.6±0.08]
NPpeg(-)	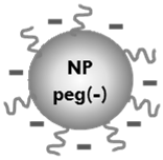	COOH+PEG	-32 mV	-55 mV	61±0 nm [0.5±0.01]	109±6 nm [0.1±0.002]
NP peg(0)	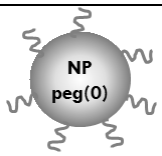	PEG	-29 mV	-99 mV	64±1 nm [0.5±0.03]	101±3 nm [0.2±0.02]
NPpeg(+)	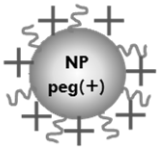	NH_2+PEG	18 mV	-92 mV	86±7 nm [0.4±0.02]	124±8 nm [0.2±0.01]
NP(+)	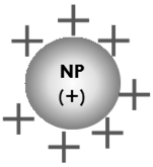	NH_2	25 mV	-109 mV	75±2 nm [0.2±0.002]	115±7 nm [0.5±0.002]

3.2. Cellular uptake

Cellular uptake of the various NP types is illustrated in Figure 2. Whatever the NP tested, cellular uptake and adsorption to cell membrane were found to be dose-dependent. The amount of NP uptaken was the most important in the case of NP free of PEG: NP(-) and NP(+) irrespectively of their charges. In addition, the amount of NP adsorbed at cell surface

was the lowest for NP coated with carboxylic groups: NP(-) and NPpeg(-) in the presence or not of PEG. It clearly appeared that NP mainly remained in the supernatant whatever the surface functionalization.

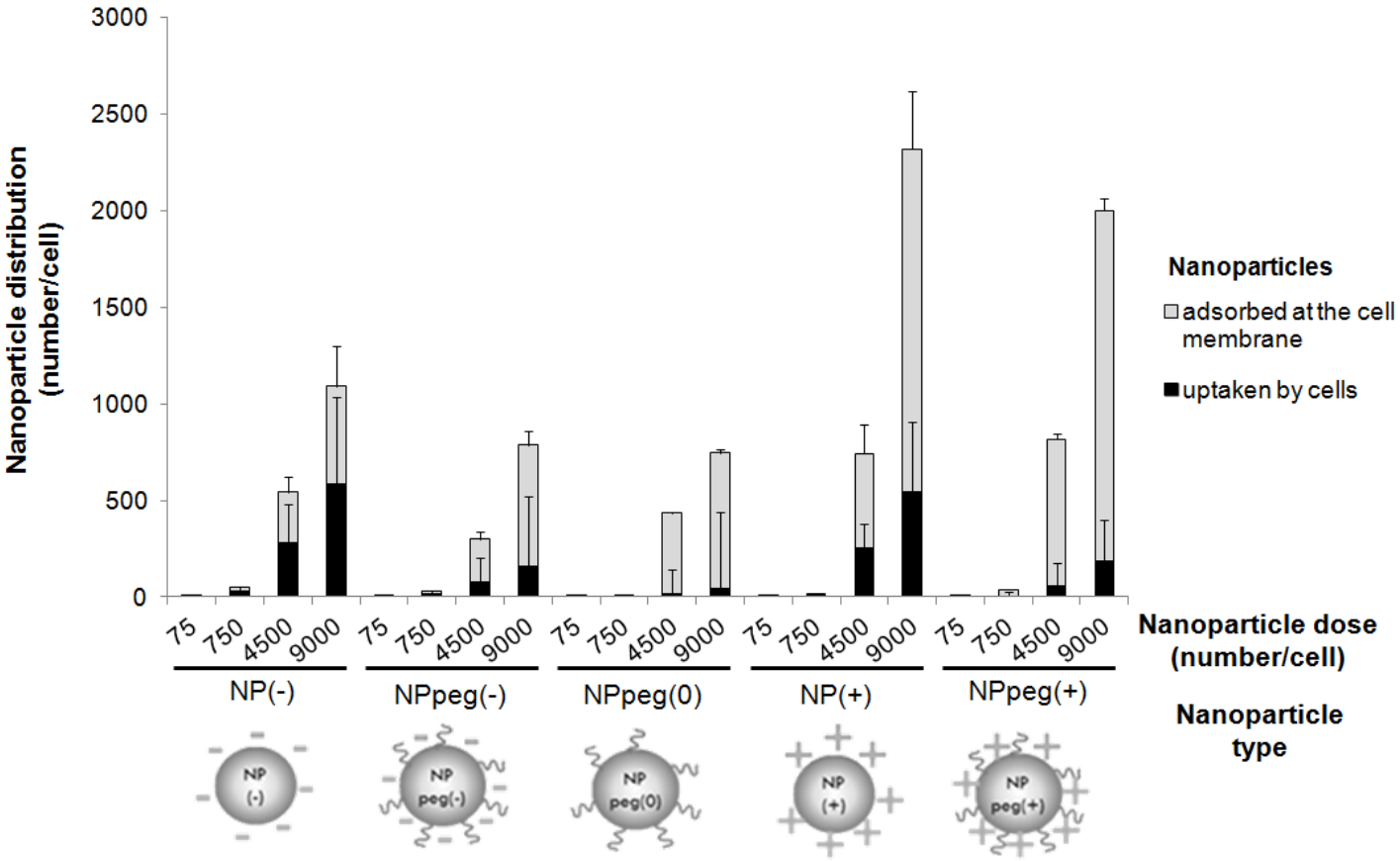

Figure 2 – Distribution of NP with different surface functionalizations. NPs were incubated with RAW264.7 for 20h, then after washing, fluorescence of cellular interacting NP was measured in presence or not of Trypan Blue. Results are means of 3 independent experiments.

3.3. Cytotoxicity assessment

Cell membrane integrity

In order to determine the cytotoxicity of the NP, LDH released in the cellular supernatant was measured after 20h of incubation. As shown by Figure 3, there was no significant difference between NP(-), NPpeg(-), NPpeg(0) and the control cells (incubated without NP) indicating

that in these conditions, the particles were not cytotoxic. Whereas NPpeg(+) were found to be cytotoxic at the dose of 600 µg/mL and NP(+) induced a release of LDH from the dose of 300 µg/mL.

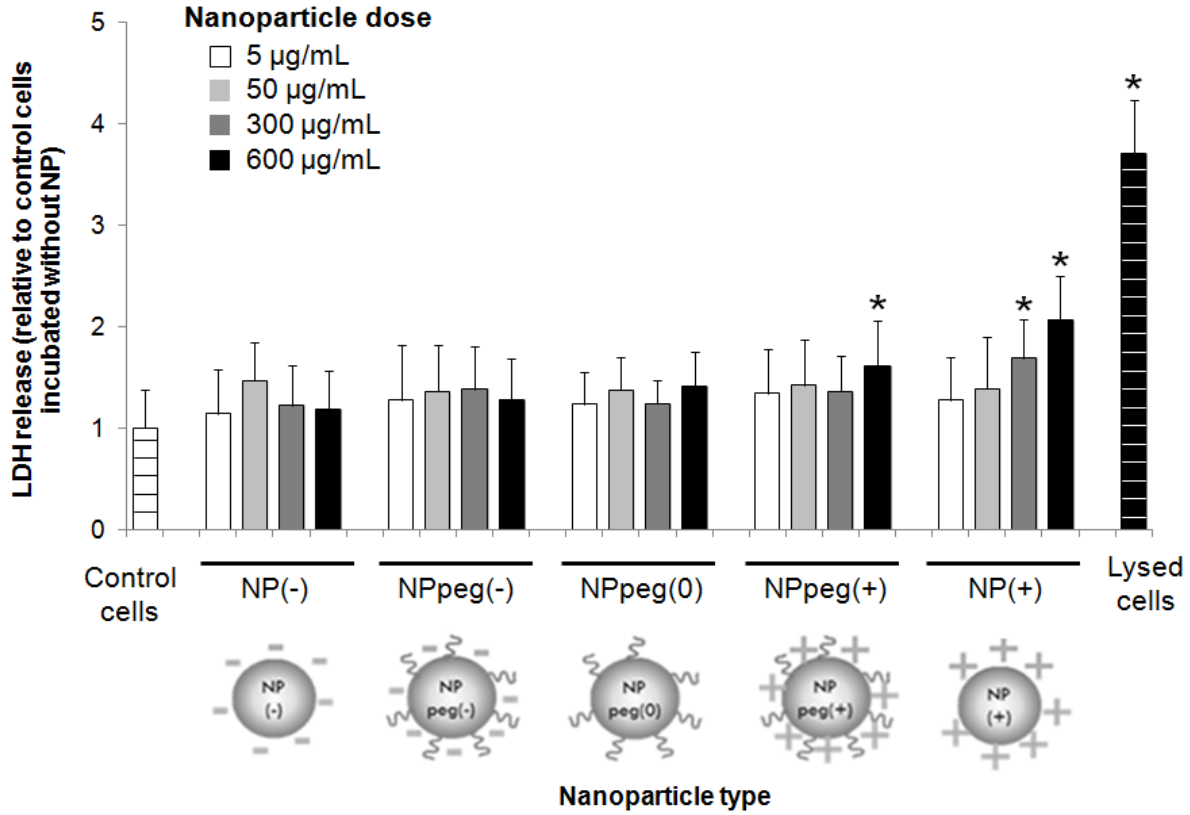

Figure 3 - Cytotoxicity of the five types of NP investigated using the LDH assay in RAW 264.7 macrophages. Results are means of 3 independent experiments. *= statistically different from negative control ($p<0.05$).

TNFα pro-inflammatory production

In order to determine if NP induced a pro-inflammatory effect, we quantified the TNFα released in the cellular supernatant. As shown in Figure 4, the amount of TNFα produced by RAW264.7 increased upon addition of the five types of NP, furthermore, the inflammatory effect was dose-dependent. NP(-) and NPpeg(-) induced the highest pro-inflammatory signal and at the highest doses this latter even exceeded the signal observed for the DQ12 positive control.

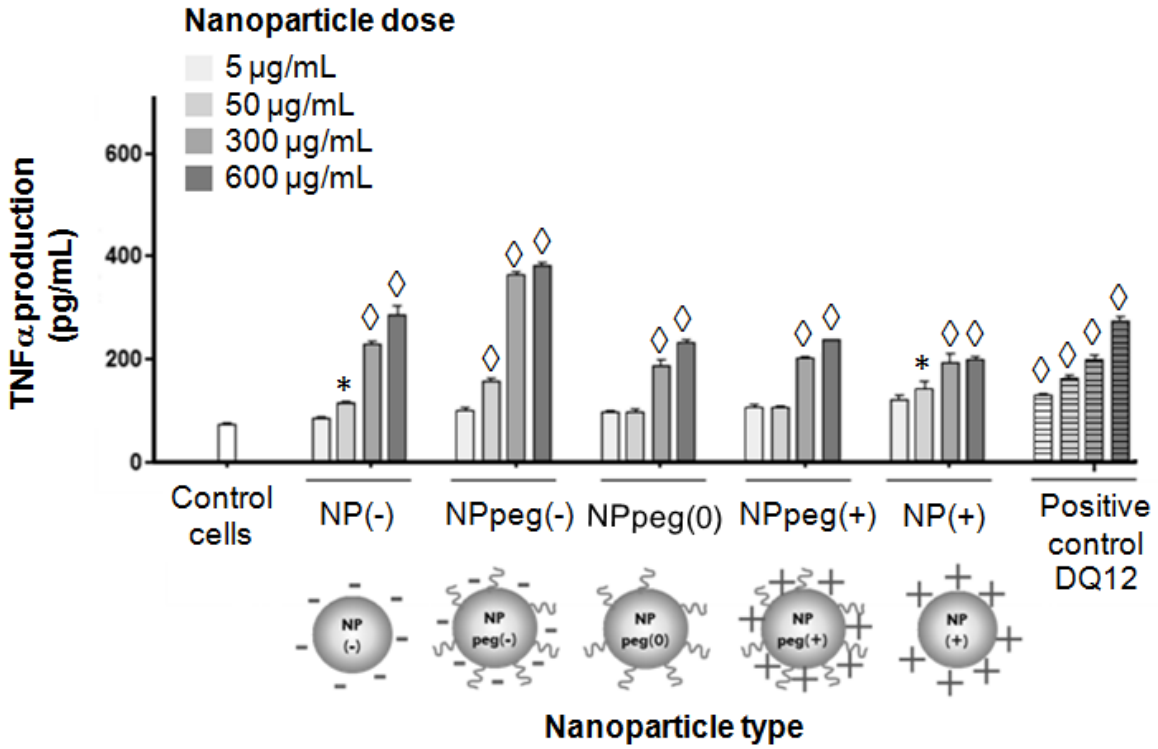

Figure 4 – Secretion of TNFα assay by RAW 264.7 macrophages in the presence of five different NP. Results are means of 3 independent experiments (*: $p<0.05$; ◊: $p<0.0001$).

Oxidative stress

No significant oxidative stress was detected when cells were incubated with the different types of NP (data not shown).

3.4. Characterization of the protein corona

It is now well established that when proteins from biological fluids are in contact with NP, they rapidly adsorb at the NP surface. In order to verify this in our model, we investigated both the amount of proteins adsorbed at the surface of NP and their nature. As shown in Figure 5, protein binding varied depending on the NP type.

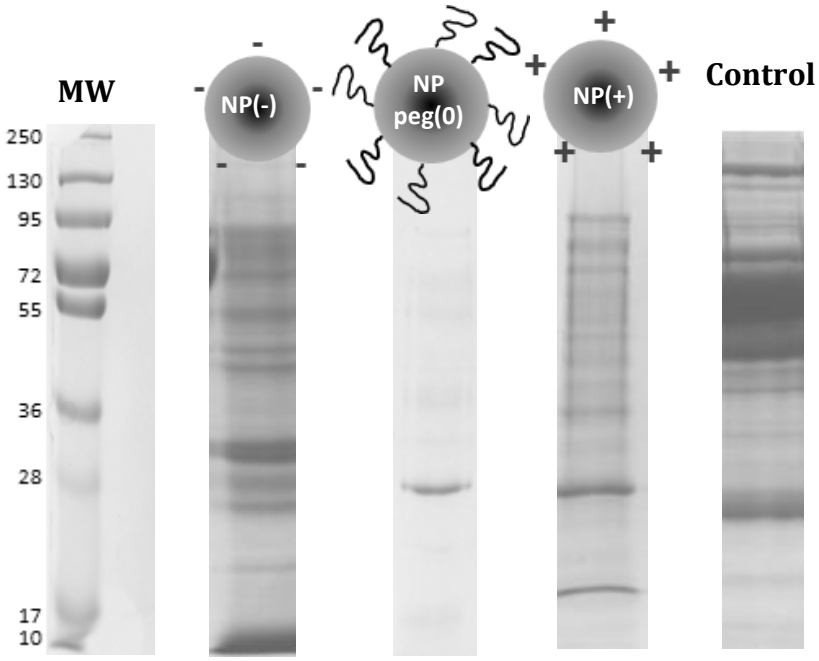

Figure 5 – SDS-PAGE gel analysis of proteins adsorbed at the surface of NP. After, incubation in the presence of human serum, NP were washed and proteins were extracted in Laemmli medium before analysis by SDS-PAGE. MW: molecular weight ladder. Human serum proteins were used as control.

As reported by Table 2, 105 proteins were characterized on NP(-) by protein mass spectroscopy, 87 and 52 on NP(+) and NPpeg(0) respectively. A qualitative analysis revealed that the nature of the proteins bound to NP(-) and NP(+) was different and only 31 proteins were found in common in both corona of NP(-) and NP(+).

Table 2 - Proteins bound to the different NP types as characterized by mass spectrometry. pI means isoelectric point.

Accession number	Protein name	NP(+)	NP(-)	NP(0)
P19652	Alpha-1-acid glycoprotein 2			X
P01009	Alpha-1-antitrypsin	X	X	X
P08697	Alpha-2-antiplasmin	X	X	
P02765	Alpha-2-HS-glycoprotein		X	X
P01023	Alpha-2-macroglobulin	X		

P03950	Angiogenin	X	X	
P01019	Angiotensinogen	X	X	
P01008	Antithrombin-III	X	X	
P02647	Apolipoprotein A-I	X	X	X
P02652	Apolipoprotein A-II	X	X	X
P06727	Apolipoprotein A-IV		X	X
P04114	Apolipoprotein B-100	X	X	
P02654	Apolipoprotein C-I	X	X	X
P02655	Apolipoprotein C-II		X	X
P02656	Apolipoprotein C-III	X	X	X
P55056	Apolipoprotein C-IV	X	X	
P05090	Apolipoprotein D		X	X
P02649	Apolipoprotein E	X	X	X
O14791	Apolipoprotein L1	X	X	
O95445	Apolipoprotein M		X	
P08519	Apolipoprotein(a)	X	X	X
P20160	Azurocidin		X	
P02749	Beta-2-glycoprotein 1	X		
P04003	C4b-binding protein alpha chain	X	X	X
P20851	C4b-binding protein beta chain	X	X	
P12830	Cadherin-1	X		
Q96IY4	Carboxypeptidase B2	X	X	
P15169	Carboxypeptidase N catalytic chain	X	X	
P49747	Cartilage oligomeric matrix protein			X
O43866	CD5 antigen-like	X		X
P00450	Ceruloplasmin		X	
P11597	Cholesteryl ester transfer protein		X	
P10909	Clusterin	X	X	X
P00740	Coagulation factor IX	X	X	
P12259	Coagulation factor V	X	X	
P08709	Coagulation factor VII		X	
P00742	Coagulation factor X	X	X	X
P03951	Coagulation factor XI	X	X	
P00748	Coagulation factor XII	X		
P00748	Coagulation factor XII	X		
P39060	Collagen alpha-1(XVIII) chain	X		
P02745	Complement C1q subcomponent subunit A	X		
P02746	Complement C1q subcomponent subunit B	X	X	
P02747	Complement C1q subcomponent subunit C	X	X	
P00736	Complement C1r subcomponent	X		
P09871	Complement C1s subcomponent	X		
P01024	Complement C3	X	X	X
P0C0L4	Complement C4	X	X	X
P01031	Complement C5	X		
P07357	Complement component C8 alpha chain	X		
P07358	Complement component C8 beta chain	X		
P07360	Complement component C8 gamma chain	X	X	
P02748	Complement component C9	X		
P02741	C-reactive protein		X	
P00751	Complement factor B	X		
P00746	Complement factor D	X		
P08603	Complement factor H	X		
Q03591	Complement factor H-related protein 1	X		

P36980	Complement factor H-related protein 2	X		
Q9BXR6	Complement factor H-related protein 5	X		
P02671	Fibrinogen alpha chain	X		X
P02675	Fibrinogen beta chain	X		X
P02679	Fibrinogen gamma chain	X		X
P02751	Fibronectin	X		
P06396	Gelsolin	X		
P04406	Glyceraldehyde-3-phosphate dehydrogenase		X	
P00738	Haptoglobin			X
P00739	Haptoglobin-related protein	X	X	
P69905	Hemoglobin subunit alpha		X	X
P68871	Hemoglobin subunit beta		X	
Q04756	Hepatocyte growth factor activator	X		
P26927	Hepatocyte growth factor-like protein	X		
P04196	Histidine-rich glycoprotein	X	X	X
Q14520	Hyaluronan-binding protein 2	X		
P01876	Ig alpha-1 chain C region	X	X	X
P01877	Ig alpha-2 chain C region		X	X
P01857	Ig gamma-1 chain C region	X	X	X
P01859	Ig gamma-2 chain C region	X	X	X
P01860	Ig gamma-3 chain C region	X		
P01861	Ig gamma-4 chain C region		X	
P01742	Ig heavy chain V-I region EU PE=1 SV=1	X		X
P01834	Ig kappa chain C region	X	X	X
P06316	Ig lambda chain V-I region BL2 PE=2 SV=1	X	X	X
P0CG04	Ig lambda-1 chain C regions	X		X
P01871	Ig mu chain C region	X	X	X
P01591	Immunoglobulin J chain	X	X	X
B9A064	Immunoglobulin lambda-like polypeptide 5	X	X	X
P01344	Insulin-like growth factor II	X	X	
P17936	Insulin-like growth factor-binding protein 3	X	X	
P24593	Insulin-like growth factor-binding protein 5	X	X	
P35858	Insulin-like growth factor-binding protein	X	X	
P19827	Inter-alpha-trypsin inhibitor heavy chain H1	X		
P19823	Inter-alpha-trypsin inhibitor heavy chain H2	X		
P29622	Kallistatin	X		
P01042	Kininogen-1	X	X	X
P02788	Lactotransferrin	X	X	
O14960	Leukocyte cell-derived chemotaxin-2	X		
P18428	Lipopolysaccharide-binding protein	X	X	
P61626	Lysozyme C	X		
P59665	Neutrophil defensin 1			X
P59666	Neutrophil defensin 3			X
P80108	PI-glycan-specific phospholipase D	X		
P03952	Plasma kallikrein	X	X	
P05155	Plasma protease C1 inhibitor	X		
P05154	Plasma serine protease inhibitor	X	X	
P00747	Plasminogen	X	X	
P02776	Platelet factor 4	X	X	X
P10720	Platelet factor 4 variant			X
P20742	Pregnancy zone protein	X		
Q15113	Procollagen C-endopeptidase enhancer 1	X		
P07737	Profilin-1	X		

P27918	Properdin	X		
P02760	Protein AMBP	X	X	X
Q9UK55	Protein Z-dependent protease inhibitor	X	X	
Q92954	Proteoglycan 4	X	X	
P00734	Prothrombin	X	X	
P62834	Ras-related protein Rap-1A		X	
P61224	Ras-related protein Rap-1b		X	
Q99969	Retinoic acid receptor responder protein 2	X		
P34096	Ribonuclease 4	X		
Q13103	Secreted phosphoprotein 24			X
P49908	Selenoprotein P	X	X	X
P02787	Serotransferrin		X	
P02768	Serum albumin	X	X	X
P0DJI8	Serum amyloid A-1 protein		X	
P0DJI9	Serum amyloid A-2 protein		X	
P35542	Serum amyloid A-4 protein	X		
P02743	Serum amyloid P-component		X	
P27169	Serum paraoxonase/arylesterase 1	X	X	
O00391	Sulfhydryl oxidase 1	X		
Q9Y490	Talin-1	X		
P05452	Tetranectin	X	X	
P07996	Thrombospondin-1		X	X
P10646	Tissue factor pathway inhibitor		X	
Q8WZ42	Titin			X
P02766	Transthyretin		X	X
Q8WUA8	Tsukushin		X	
P04070	Vitamin K-dependent protein C		X	X
P07225	Vitamin K-dependent protein S		X	X
P22891	Vitamin K-dependent protein Z		X	X
P04004	Vitronectin	X	X	X
	Total proteins number	**105**	**87**	**52**
	Complement proteins number	21	8	3
	Theoretical pI (mean value of total proteins)	6.9	6.7	6.3
	Minimum theoretical pI among the total proteins	3.9	4.5	3.9
	Maximum theoretical pI among the total proteins	11.7	9.7	9.2

4. DISCUSSION

This study aimed at understanding the relationship between surface chemical functionalizations of 50 nm silica-based NP, their ability to be uptaken by macrophages and their toxicity. First, NP were thoroughly characterized (Table 1) and it was observed that, compared to results obtained when NP were incubated in water, the hydrodynamic diameter of each type of NP increased in culture medium and zeta potentials became negative, all the more so important if NP were non-pegylated (NP(-) and NP(+)). This is consistent with

literature data reporting that initially positively charged NP can turn negative when incubated with serum [30,42]. This tendency was observed with different types of NP such as polystyrene [25], gold [43], silica [23] or magnetic NP [32]. This alteration is very likely due to the formation of a protein corona [19,21,23,44], indeed, adsorbed proteins can hide chemical groups initially grafted onto the NP surface, NP surface charge is thus modified and rather related to the nature of the adsorbed proteins. In our model, the analysis of the protein corona of NP (Figure 5) allowed to detect the lowest number of proteins on the NPpeg(0) which is likely due to the steric hindrance caused by the long PEG chains.

Then, to investigate the influence of NP surface functionalization on NP/cell interactions, NP were incubated with macrophages and their phagocytosis was quantified (Figure 2). Interestingly, non-pegylated (NP(-) and NP(+)) were the most uptaken by cells, whereas, independently of PEG coating, NPpeg(+) and NP(+) were the most adsorbed at the macrophage cell surface. This suggests that while NP uptake might be related to the absence of PEG grafting, NP adsorption at the cell membrane might rather be correlated to the initially positively charged NP surface. It involves a close relationship between NP surface functionalization, the protein corona and interaction with cells. The presence of a protein corona seems to foster cellular uptake. It has already been reported that pegylation, by preventing protein adsorption at the NP surface, results in limited NP internalization [8,24]. These data are also in agreement with results from Qiu *et al.* who demonstrated that gold nanorods exhibiting the highest adsorption capability for proteins also showed the highest internalization [30]. Similarly, magnetic NP were more rapidly and more abundantly internalized by cells after formation of the protein corona [32]. As previously suggested, specific parts of the proteins covering NP could be recognized by membrane receptors thus facilitating their internalization [1,30,45].

But others reported that a protein corona may inhibit NP uptake [18,19,29,31]. For instance, Lesniak *et al.* have shown that lung epithelial cells internalized more rapidly and in larger quantities 50 nm silica NP incubated in culture medium without serum than after addition of 10% serum [46]. One hypothesis to explain these discrepancies may lie in different pathways of cell internalization. Therefore, depending on the presence or absence of a protein corona the uptake mechanism might be different. Indeed, cellular internalization can occur through specific or non-specific pathways, in the first case, it involves receptors located at the plasma membrane which are activated by specific ligands [1]. For instance, Saptarshi *et al.* observed that NH_2-polystyrene NP uptake by macrophages in a protein free medium was changed from clathrin-mediated endocytosis to phagocytosis when incubated in serum enriched media [29].

Many authors have reported that high adsorption of positively charged NP may be related to electrostatic interactions with the negatively charged cell surface [47]. But it should be kept in mind that zeta potentials of all types of NP turned negative in culture medium, therefore a different explanation may be envisaged in relation with the protein corona formation: the positively charged NP might be covered with specific proteins which fostered NP adsorption at the cell membrane through interaction with receptors as it was previously mentioned [1,30,45].

By altering NP /cell interactions, the formation of a protein corona can have a deep impact on the cellular response. The investigation of the cytotoxicity induced by the different types of NP revealed that only initially positively charged NP triggered a significant loss of cell membrane integrity (Figure 3) but solely at the highest doses (from 300 or 600µg/mL for NP(+) and NPpeg(+) respectively). It is important to note that these concentrations are very high and are not representative of what the cells might be exposed to in the organism, but these concentrations were necessary to characterize NP distribution, lower doses did not lead to discriminating results. Although the five types of NP were able to enhance TNFα

production at high doses, NP(-) and NPpeg(-) induced the highest levels (Figure 4). No significant oxidative stress was detected which is consistent with similar studies carried out by Panas *et al.* where the same RAW264.7 macrophages were incubated with engineered silica NP of 25 nm diameter [48].

It is quite challenging to precisely characterize the composition of a protein corona because of its complex and dynamic nature [49]. However simple SDS-PAGE gel electrophoresis of desorbed proteins from NP previously incubated in a culture medium supplemented with serum can give some interesting insights. Our study on the protein corona allowed concluding that: 1) the profile of protein binding was different depending on NP surface functionalization (Figure 5) with many proteins of different nature adsorbed on NP(-), NP(+) and to a less degree on NPpeg(0) because of the steric hindrance provided by PEG; and 2) the corona composition did not reflect the relative abundance of the proteins in the surrounding medium. This absence of correlation has already been reported [18,50] and it has been suggested to depend on the NP physico-chemical features [29]. For example, albumin and apolipoprotein AI et II, C and E were found, in variable quantities, on the three types of NP, similar results were obtained by Izak-Nau *et al.* who analyzed the protein corona of 50 nm silica NP functionalized either with amine, thiol or polyvinylpyrrolidone groups after incubation in DMEM medium supplemented with 10% bovine or human serum [20] whereas many proteins were found on only one type of NP. The quantitative aspect should also be distinguished from the qualitative one, as in terms of biological response, the more abundantly associated proteins do not necessarily have the most profound effect and as a corollary, a less abundant protein with high affinity may instead play a major role [18,44]. Interestingly, among the 23 complement components characterized in the protein corona of the tested NP (proteins in gray in Table 2), 21 were found on NP(+) and only 8 and 3 on NP(-) and NPpeg(0) respectively, corresponding to 20 %, 9 % and 6% of the proteins identified on these NP. The mean value of

theoretical pI of proteins characterized on NP(+) was 6.9 (max 11.7 and min 3.9) whereas for NP(-) it was 6.7 (max 9.7, min 4.5), this calculation did not take into account the respective quantity of the proteins (see Table 2). It suggests that protein binding to NP was not linked to their theoretical charges. In addition, Izak-Nau *et al.* demonstrated also that the protein corona evolved with time and that proteins preferentially adsorbed on NP surface at a specific time point can be associated with another type of NP at another time of analysis [20].

Moreover, the protein corona formation depends on many parameters. For example, NP coating with proteins is specific of the biological environment and thus of the *in vitro* culture conditions. Beyond the composition of the culture medium it involves parameters such as pH, ionic strength, salt concentrations, etc. Finally, the type of NP functionalization should also be taken into account. As an example, Graf *et al.* reported that one type of positively charged particle (AHAPS) was easily internalized by macrophages, while another type of positively charged particle (short alkyl chain aminosilanes) was uptaken by cells in a lower amount, this could be due to a difference of functionalization in group types and density. Similarly, it was observed that the uptake efficiency of PEGylated NP was closely related to PEG grafting density and molecular architecture of PEG [8,24,51].

5. CONCLUSIONS

In conclusion, the present study demonstrated that surface chemical functionalization plays a key role in the interactions between silica-based NP and cells. Interestingly, NP uptake by phagocytic cells seems to be related to the absence of PEG, while the NP adsorption at the cell membrane seems to be influenced by an initial positively charged NP surface. Moreover, the biological *in vitro* toxicity was not correlated with NP uptake. This study also underscores the major role of the protein corona and clearly argues for its systematic consideration in

nanotoxicology studies as it defines the biological identity of the NP and directly influences interactions with cells and the subsequent biological outcome. Therefore a better knowledge of the relationship between the initial NP physico-chemical properties, the protein corona and cellular uptake efficiency could guide the design of NP either in a therapeutic perspective (development of new nanodevices with enhanced cellular uptake) or in the context of safety issues (safer by design synthesis of NP).

ACKNOWLEDGEMENTS

The authors would like to acknowledge the Région Rhône-Alpes and the Conseil Général de la Loire for financial support.

REFERENCES

[1] F. Zhao, Y. Zhao, Y. Liu, X. Chang, C. Chen, Y. Zhao, Cellular uptake, intracellular trafficking, and cytotoxicity of nanomaterials, Small Weinh. Bergstr. Ger. 7 (2011) 1322–1337. doi:10.1002/smll.201100001.

[2] A. Albanese, P.S. Tang, W.C.W. Chan, The effect of nanoparticle size, shape, and surface chemistry on biological systems, Annu. Rev. Biomed. Eng. 14 (2012) 1–16. doi:10.1146/annurev-bioeng-071811-150124.

[3] T.-H. Chung, S.-H. Wu, M. Yao, C.-W. Lu, Y.-S. Lin, Y. Hung, C.-Y. Mou, Y.-C. Chen, D.-M. Huang, The effect of surface charge on the uptake and biological function of mesoporous silica nanoparticles in 3T3-L1 cells and human mesenchymal stem cells, Biomaterials. 28 (2007) 2959–2966. doi:10.1016/j.biomaterials.2007.03.006.

[4] S. Patil, A. Sandberg, E. Heckert, W. Self, S. Seal, Protein adsorption and cellular uptake of cerium oxide nanoparticles as a function of zeta potential, Biomaterials. 28 (2007) 4600–4607. doi:10.1016/j.biomaterials.2007.07.029.

[5] S. Kralj, M. Rojnik, R. Romih, M. Jagodič, J. Kos, D. Makovec, Effect of surface charge on the cellular uptake of fluorescent magnetic nanoparticles, J. Nanoparticle Res. 14 (2012) 1–14. doi:10.1007/s11051-012-1151-7.

[6] C. Schweiger, R. Hartmann, F. Zhang, W.J. Parak, T.H. Kissel, P. Rivera_Gil, Quantification of the internalization patterns of superparamagnetic iron oxide nanoparticles with opposite charge, J. Nanobiotechnology. 10 (2012) 1–11. doi:10.1186/1477-3155-10-28.

[7] C. He, Y. Hu, L. Yin, C. Tang, C. Yin, Effects of particle size and surface charge on cellular uptake and biodistribution of polymeric nanoparticles, Biomaterials. 31 (2010) 3657–3666. doi:10.1016/j.biomaterials.2010.01.065.

[8] A. Verma, F. Stellacci, Effect of surface properties on nanoparticle-cell interactions, Small Weinh. Bergstr. Ger. 6 (2010) 12–21. doi:10.1002/smll.200901158.

[9] S.-H. Yang, D. Heo, J. Park, S. Na, J.-S. Suh, S. Haam, S.W. Park, Y.-M. Huh, J. Yang, Role of surface charge in cytotoxicity of charged manganese ferrite nanoparticles towards macrophages, Nanotechnology. 23 (2012) 505702. doi:10.1088/0957-4484/23/50/505702.

[10] Z.-G. Yue, W. Wei, P.-P. Lv, H. Yue, L.-Y. Wang, Z.-G. Su, G.-H. Ma, Surface charge affects cellular uptake and intracellular trafficking of chitosan-based nanoparticles, Biomacromolecules. 12 (2011) 2440–2446. doi:10.1021/bm101482r.

[11] S.T. Kim, K. Saha, C. Kim, V.M. Rotello, The role of surface functionality in determining nanoparticle cytotoxicity, Acc. Chem. Res. 46 (2013) 681–691. doi:10.1021/ar3000647.

[12] T. Yu, A. Malugin, H. Ghandehari, Impact of silica nanoparticle design on cellular toxicity and hemolytic activity, ACS Nano. 5 (2011) 5717–5728. doi:10.1021/nn2013904.

[13] K. Greish, G. Thiagarajan, H. Herd, R. Price, H. Bauer, D. Hubbard, A. Burckle, S. Sadekar, T. Yu, A. Anwar, A. Ray, H. Ghandehari, Size and surface charge significantly influence the toxicity of silica and dendritic nanoparticles, Nanotoxicology. 6 (2012) 713–723. doi:10.3109/17435390.2011.604442.

[14] E. Fröhlich, The role of surface charge in cellular uptake and cytotoxicity of medical nanoparticles, Int. J. Nanomedicine. 7 (2012) 5577–5591. doi:10.2147/IJN.S36111.

[15] H. Nabeshi, T. Yoshikawa, A. Arimori, T. Yoshida, S. Tochigi, T. Hirai, T. Akase, K. Nagano, Y. Abe, H. Kamada, S.-I. Tsunoda, N. Itoh, Y. Yoshioka, Y. Tsutsumi, Effect of surface properties of silica nanoparticles on their cytotoxicity and cellular distribution in murine macrophages, Nanoscale Res. Lett. 6 (2011) 93. doi:10.1186/1556-276X-6-93.

[16] V. Chandolu, C.R. Dass, Treatment of lung cancer using nanoparticle drug delivery systems, Curr. Drug Discov. Technol. 10 (2013) 170–176.

[17] A. Mignot, C. Truillet, F. Lux, L. Sancey, C. Louis, F. Denat, F. Boschetti, L. Bocher, A. Gloter, O. Stéphan, R. Antoine, P. Dugourd, D. Luneau, G. Novitchi, L.C. Figueiredo, P.C. de Morais, L. Bonneviot, B. Albela, F. Ribot, L. Van Lokeren, I. Déchamps-Olivier, F. Chuburu, G. Lemercier, C. Villiers, P.N. Marche, G. Le Duc, S. Roux, O. Tillement, P. Perriat, A top-down synthesis route to ultrasmall multifunctional Gd-based silica nanoparticles for theranostic applications, Chem. Weinh. Bergstr. Ger. 19 (2013) 6122–6136. doi:10.1002/chem.201203003.

[18] E. Brun, C. Sicard-Roselli, Could nanoparticle corona characterization help for biological consequence prediction?, Cancer Nanotechnol. 5 (2014) 7. doi:10.1186/s12645-014-0007-5.

[19] D. Docter, C. Bantz, D. Westmeier, H.J. Galla, Q. Wang, J.C. Kirkpatrick, P. Nielsen, M. Maskos, R.H. Stauber, The protein corona protects against size- and dose-dependent

toxicity of amorphous silica nanoparticles, Beilstein J. Nanotechnol. 5 (2014) 1380–1392. doi:10.3762/bjnano.5.151.

[20] E. Izak-Nau, M. Voetz, S. Eiden, A. Duschl, V.F. Puntes, Altered characteristics of silica nanoparticles in bovine and human serum: the importance of nanomaterial characterization prior to its toxicological evaluation, Part. Fibre Toxicol. 10 (2013) 56. doi:10.1186/1743-8977-10-56.

[21] I. Lynch, K.A. Dawson, Protein-nanoparticle interactions, Nano Today. 3 (2008) 40–47. doi:10.1016/S1748-0132(08)70014-8.

[22] M.P. Monopoli, C. Aberg, A. Salvati, K.A. Dawson, Biomolecular coronas provide the biological identity of nanosized materials, Nat. Nanotechnol. 7 (2012) 779–786. doi:10.1038/nnano.2012.207.

[23] N.P. Mortensen, G.B. Hurst, W. Wang, C.M. Foster, P.D. Nallathamby, S.T. Retterer, Dynamic development of the protein corona on silica nanoparticles: composition and role in toxicity, Nanoscale. 5 (2013) 6372–6380. doi:10.1039/C3NR33280B.

[24] C. Cruje, D.B. Chithrani, Polyethylene Glycol Density and Length Affects Nanoparticle Uptake by Cancer Cells, J. Nanomedicine Res. 1 (2014). doi:10.15406/jnmr.2014.01.00006.

[25] M.S. Ehrenberg, A.E. Friedman, J.N. Finkelstein, G. Oberdörster, J.L. McGrath, The influence of protein adsorption on nanoparticle association with cultured endothelial cells, Biomaterials. 30 (2009) 603–610. doi:10.1016/j.biomaterials.2008.09.050.

[26] P. Aggarwal, J.B. Hall, C.B. McLeland, M.A. Dobrovolskaia, S.E. McNeil, Nanoparticle interaction with plasma proteins as it relates to particle biodistribution, biocompatibility and therapeutic efficacy, Adv. Drug Deliv. Rev. 61 (2009) 428–437. doi:10.1016/j.addr.2009.03.009.

[27] C.D. Walkey, J.B. Olsen, H. Guo, A. Emili, W.C.W. Chan, Nanoparticle Size and Surface Chemistry Determine Serum Protein Adsorption and Macrophage Uptake, J. Am. Chem. Soc. 134 (2012) 2139–2147. doi:10.1021/ja2084338.

[28] C.D. Walkey, W.C.W. Chan, Understanding and controlling the interaction of nanomaterials with proteins in a physiological environment, Chem. Soc. Rev. 41 (2012) 2780–2799. doi:10.1039/c1cs15233e.

[29] S.R. Saptarshi, A. Duschl, A.L. Lopata, Interaction of nanoparticles with proteins: relation to bio-reactivity of the nanoparticle, J. Nanobiotechnology. 11 (2013) 26. doi:10.1186/1477-3155-11-26.

[30] Y. Qiu, Y. Liu, L. Wang, L. Xu, R. Bai, Y. Ji, X. Wu, Y. Zhao, Y. Li, C. Chen, Surface chemistry and aspect ratio mediated cellular uptake of Au nanorods, Biomaterials. 31 (2010) 7606–7619. doi:10.1016/j.biomaterials.2010.06.051.

[31] A. Lesniak, A. Campbell, M.P. Monopoli, I. Lynch, A. Salvati, K.A. Dawson, Serum heat inactivation affects protein corona composition and nanoparticle uptake, Biomaterials. 31 (2010) 9511–9518. doi:10.1016/j.biomaterials.2010.09.049.

[32] M.M. Yallapu, N. Chauhan, S.F. Othman, V. Khalilzad-Sharghi, M.C. Ebeling, S. Khan, M. Jaggi, S.C. Chauhan, Implications of protein corona on physico-chemical and biological properties of magnetic nanoparticles, Biomaterials. 46 (2015) 1–12. doi:10.1016/j.biomaterials.2014.12.045.

[33] M. Martini, P. Perriat, M. Montagna, R. Pansu, C. Julien, O. Tillement, S. Roux, How Gold Particles Suppress Concentration Quenching of Fluorophores Encapsulated in Silica Beads, J. Phys. Chem. C. 113 (2009) 17669–17677. doi:10.1021/jp9044572.

[34] E.S. Van Amersfoort, J.A. Van Strijp, Evaluation of a flow cytometric fluorescence quenching assay of phagocytosis of sensitized sheep erythrocytes by polymorphonuclear leukocytes, Cytometry. 17 (1994) 294–301. doi:10.1002/cyto.990170404.

[35] J. Nuutila, E.-M. Lilius, Flow cytometric quantitative determination of ingestion by phagocytes needs the distinguishing of overlapping populations of binding and ingesting cells, Cytom. Part J. Int. Soc. Anal. Cytol. 65 (2005) 93–102. doi:10.1002/cyto.a.20139.

[36] L. Leclerc, D. Boudard, J. Pourchez, V. Forest, O. Sabido, V. Bin, S. Palle, P. Grosseau, D. Bernache, M. Cottier, Quantification of microsized fluorescent particles phagocytosis to a better knowledge of toxicity mechanisms, Inhal. Toxicol. 22 (2010) 1091–1100. doi:10.3109/08958378.2010.522781.

[37] A. Kurtz-Chalot, J.P. Klein, J. Pourchez, D. Boudard, V. Bin, G.B. Alcantara, M. Martini, M. Cottier, V. Forest, Adsorption at cell surface and cellular uptake of silica nanoparticles with different surface chemical functionalizations: impact on cytotoxicity, J. Nanoparticle Res. 16 (2014) 1–15. doi:10.1007/s11051-014-2738-y.

[38] A. Kurtz-Chalot, J.-P. Klein, J. Pourchez, D. Boudard, V. Bin, O. Sabido, L. Marmuse, M. Cottier, V. Forest, Quantification of nanoparticle endocytosis based on double fluorescent pH-sensitive nanoparticles, Biomed. Microdevices. 17 (2015) 9947. doi:10.1007/s10544-015-9947-8.

[39] S.E.A. Gratton, P.A. Ropp, P.D. Pohlhaus, J.C. Luft, V.J. Madden, M.E. Napier, J.M. DeSimone, The effect of particle design on cellular internalization pathways, Proc. Natl. Acad. Sci. U. S. A. 105 (2008) 11613–11618. doi:10.1073/pnas.0801763105.

[40] J. Bruch, S. Rehn, B. Rehn, P.J.A. Borm, B. Fubini, Variation of biological responses to different respirable quartz flours determined by a vector model, Int. J. Hyg. Environ. Health. 207 (2004) 203–216. doi:10.1078/1438-4639-00278.

[41] B. Fubini, I. Fenoglio, R. Ceschino, M. Ghiazza, G. Martra, M. Tomatis, P. Borm, R. Schins, J. Bruch, Relationship between the state of the surface of four commercial quartz flours and their biological activity in vitro and in vivo, Int. J. Hyg. Environ. Health. 207 (2004) 89–104. doi:10.1078/1438-4639-00277.

[42] M. Lundqvist, J. Stigler, G. Elia, I. Lynch, T. Cedervall, K.A. Dawson, Nanoparticle size and surface properties determine the protein corona with possible implications for biological impacts, Proc. Natl. Acad. Sci. U. S. A. 105 (2008) 14265–14270. doi:10.1073/pnas.0805135105.

[43] I.A. Pyshnaya, K.V. Razum, J.E. Poletaeva, D.V. Pyshnyi, M.A. Zenkova, E.I. Ryabchikova, Comparison of behaviour in different liquids and in cells of gold nanorods and spherical nanoparticles modified by linear polyethyleneimine and bovine serum albumin, BioMed Res. Int. 2014 (2014) 908175. doi:10.1155/2014/908175.

[44] T. Cedervall, I. Lynch, S. Lindman, T. Berggård, E. Thulin, H. Nilsson, K.A. Dawson, S. Linse, Understanding the nanoparticle-protein corona using methods to quantify exchange rates and affinities of proteins for nanoparticles, Proc. Natl. Acad. Sci. U. S. A. 104 (2007) 2050–2055. doi:10.1073/pnas.0608582104.

[45] V. Forest, M. Cottier, J. Pourchez, Electrostatic interactions favor the binding of positive nanoparticles on cells: A reductive theory, Nano Today. (n.d.). doi:10.1016/j.nantod.2015.07.002.

[46] A. Lesniak, F. Fenaroli, M.P. Monopoli, C. Åberg, K.A. Dawson, A. Salvati, Effects of the presence or absence of a protein corona on silica nanoparticle uptake and impact on cells, ACS Nano. 6 (2012) 5845–5857. doi:10.1021/nn300223w.

[47] A.M. El Badawy, R.G. Silva, B. Morris, K.G. Scheckel, M.T. Suidan, T.M. Tolaymat, Surface charge-dependent toxicity of silver nanoparticles, Environ. Sci. Technol. 45 (2011) 283–287. doi:10.1021/es1034188.

[48] A. Panas, C. Marquardt, O. Nalcaci, H. Bockhorn, W. Baumann, H.-R. Paur, S. Mülhopt, S. Diabaté, C. Weiss, Screening of different metal oxide nanoparticles reveals selective toxicity and inflammatory potential of silica nanoparticles in lung epithelial

cells and macrophages, Nanotoxicology. 7 (2013) 259–273. doi:10.3109/17435390.2011.652206.

[49] M.A. Dobrovolskaia, B.W. Neun, S. Man, X. Ye, M. Hansen, A.K. Patri, R.M. Crist, S.E. McNeil, Protein corona composition does not accurately predict hematocompatibility of colloidal gold nanoparticles, Nanomedicine Nanotechnol. Biol. Med. 10 (2014) 1453–1463. doi:10.1016/j.nano.2014.01.009.

[50] G. Maiorano, S. Sabella, B. Sorce, V. Brunetti, M.A. Malvindi, R. Cingolani, P.P. Pompa, Effects of Cell Culture Media on the Dynamic Formation of Protein−Nanoparticle Complexes and Influence on the Cellular Response, ACS Nano. 4 (2010) 7481–7491. doi:10.1021/nn101557e.

[51] C. Graf, Q. Gao, I. Schütz, C.N. Noufele, W. Ruan, U. Posselt, E. Korotianskiy, D. Nordmeyer, F. Rancan, S. Hadam, A. Vogt, J. Lademann, V. Haucke, E. Rühl, Surface functionalization of silica nanoparticles supports colloidal stability in physiological media and facilitates internalization in cells, Langmuir ACS J. Surf. Colloids. 28 (2012) 7598–7613. doi:10.1021/la204913t.